

Supporting Information

α -hub domains: from structure, stability and binding to selection in transcriptional interactomes

Frederik Friis Theisen^{1#}, Edoardo Salladini[#], Rikke Davidsen¹, Christina Jo Rasmussen¹, Lasse Staby¹², Birthe B. Kragelund^{12*} and Karen Skriver^{1*}

¹ REPIN and the Linderstrøm-Lang Centre for Protein Science, Department of Biology, University of Copenhagen, Copenhagen, DK-2200, Denmark

² Structural Biology and NMR Laboratory, Department of Biology, University of Copenhagen, Copenhagen, Denmark

These authors contributed equally to this work

* Correspondence: Birthe B. Kragelund, bbk@bio.ku.dk; Karen Skriver, kskriver@bio.ku.dk

Running title: *α -hubs: correlating structure, stability and interactome*

List of contents:

S-2: Table S1 SAXS data collection and derived parameters for *At*TAF4-RST

S-2: Table S2 R_g (from Guinier) and D_{max} for the *At*TAF4-RST domain at various protein concentrations

S-3: Table S3 NMR refinement statistics for *At*TAF4-RST

S-3: Table S4 Parameters from denaturation experiments

S-4: Figure S1 SAXS studies of *At*TAF4-RST

S-5: Figure S2 Dynamics of *At*TAF4-RST

S-6: Figure S3 Stabilities of the *At*RCD1-RST, *At*TAF4-RST and *Hs*TAF4-TAFH domains

S-7: Figure S4 HSQC spectra of thermal unfolding of RST from *At*TAF4 and *At*RCD1

S-8: Figure S5 ITC measurements at different temperatures

S-9: Figure S6 HSQC spectra of free and *At*TAF4-RST bound DREB2A

S-9: References

TABLE S1

SAXS data collection and derived parameters for *AfTAF4-RST*

Data-collection parameters	
Data source and instrument (beamline)	Hamburg (P12)
Instrument (detector)	PILATUS 6M
Beam geometry (mm ²)	0.2 x 0.12
Wavelength (Å)	1.239
Detector distance (m)	3
<i>s</i> range (nm ⁻¹)	0.025 - 7.317
Exposure time (sec)	0.5 (50 x 0.01)
Concentration range (mg ml ⁻¹)	1.12 – 8.93
Temperature (K)	293
Structural parameters	
<i>I</i> (0) (cm ⁻¹) [from <i>P</i> (<i>r</i>) of normalized samples]	13.8 ± 0.1
<i>R_g</i> (Å) [from <i>P</i> (<i>r</i>)]	15.4 ± 0.4
<i>I</i> (0) (cm ⁻¹) [from Guinier approximation of normalized samples]	13.7 ± 0.1
<i>R_g</i> (Å) [from Guinier approximation]	15.4 ± 0.1
<i>D_{max}</i> (Å)	45.0 ± 1.2
Molecular-mass determination	
Molecular mass <i>M_r</i> (kDa) [from <i>water calibration</i>]	8.56 ± 0.23
Calculated monomeric <i>M_r</i> (kDa) [from <i>sequence</i>]*	8.65
Software employed	
Primary data reduction	PRIMUS
Data processing	PRIMUS
<i>Ab initio</i> analysis	DAMMIF
Validation and averaging	DAMAVR
Computation of model intensities	CRYSOL

* Obtained using the ProtParam tool of the Expasy server (<https://web.expasy.org/protparam/>).

TABLE S2

R_g and *D_{max}* for the *AfTAF4-RST* domain at different concentrations

[TAF4] (g L ⁻¹)	MW (Guinier) (kDa)	<i>R_g</i> (Guinier) (Å)	<i>R_g</i> (<i>P</i> (<i>r</i>)) (Å)	<i>D_{max}</i> (Å)
1.12	7.3 ± 0.7	15.0 ± 0.1	15.1	40.9
2.14	8.5 ± 0.2	15.3 ± 0.1	15.2	43.6
2.59	8.8 ± 0.1	15.3 ± 0.1	15.2	44.8
3.65	9.1 ± 0.1	15.7 ± 0.4	15.3	44.0
4.20	8.6 ± 0.5	15.5 ± 0.1	15.4	45.3
8.93	8.5 ± 1.3	15.8 ± 0.1	15.9	51.3

* The expected MW in kDa is 8.9.

TABLE S3**NMR refinement statistics for *At*TAF4-RST**

		<i>At</i> TAF4-RST
NMR distance restraints and dihedral constraints		
Distance restraints		
Total NOEs		1248
Intra-residue		285
Inter-residue		963
Sequential ($ i - j = 1$)		307
Medium-range ($ i - j \leq 5$)		362
Long-range ($ i - j > 5$)		294
Hydrogen bonds		0
Total dihedral angle constraints		116
ϕ		58
ψ		58
Structure statistics		
Violations (mean \pm sd)		
Distance constraints (\AA)		0.025 ± 0.002
Dihedral angle constraints ($^\circ$)		0.213 ± 0.105
Max. dihedral angle violations ($^\circ$)		2.41
Max. distance constraint violation (\AA)		0.431
Deviations from idealized geometry		
Bond lengths (\AA)		0.006 ± 0.000
Bond angles ($^\circ$)		0.852 ± 0.006
Impropers ($^\circ$)		0.494 ± 0.011
Average pairwise r.m.s. deviation (\AA)		
Heavy (193-250)		1.07 ± 0.14
Backbone (193-250)		0.25 ± 0.07
Ramachandran plot statistics (%)		
Residues in most favored regions		99.2
Residues in additionally allowed regions		0.8
Residues in generously allowed regions		0.0
Residues in disallowed regions		0.0

TABLE S4**Parameters from denaturation experiments**

	$\Delta H_{\text{VH}}/\Delta H_{\text{m}}$	C_m (M) (CD chemical denaturation)	C_m (M) (Two-dimensional global analysis)
<i>At</i> RCD1-RST	0.5	2.6 ± 0.2	2.59 ± 0.01
<i>At</i> TAF4-RST	0.4	1.9 ± 0.6	1.74 ± 0.09
<i>Hs</i> TAF4-TAFH	0.3	2.4 ± 0.1	3.18 ± 0.03

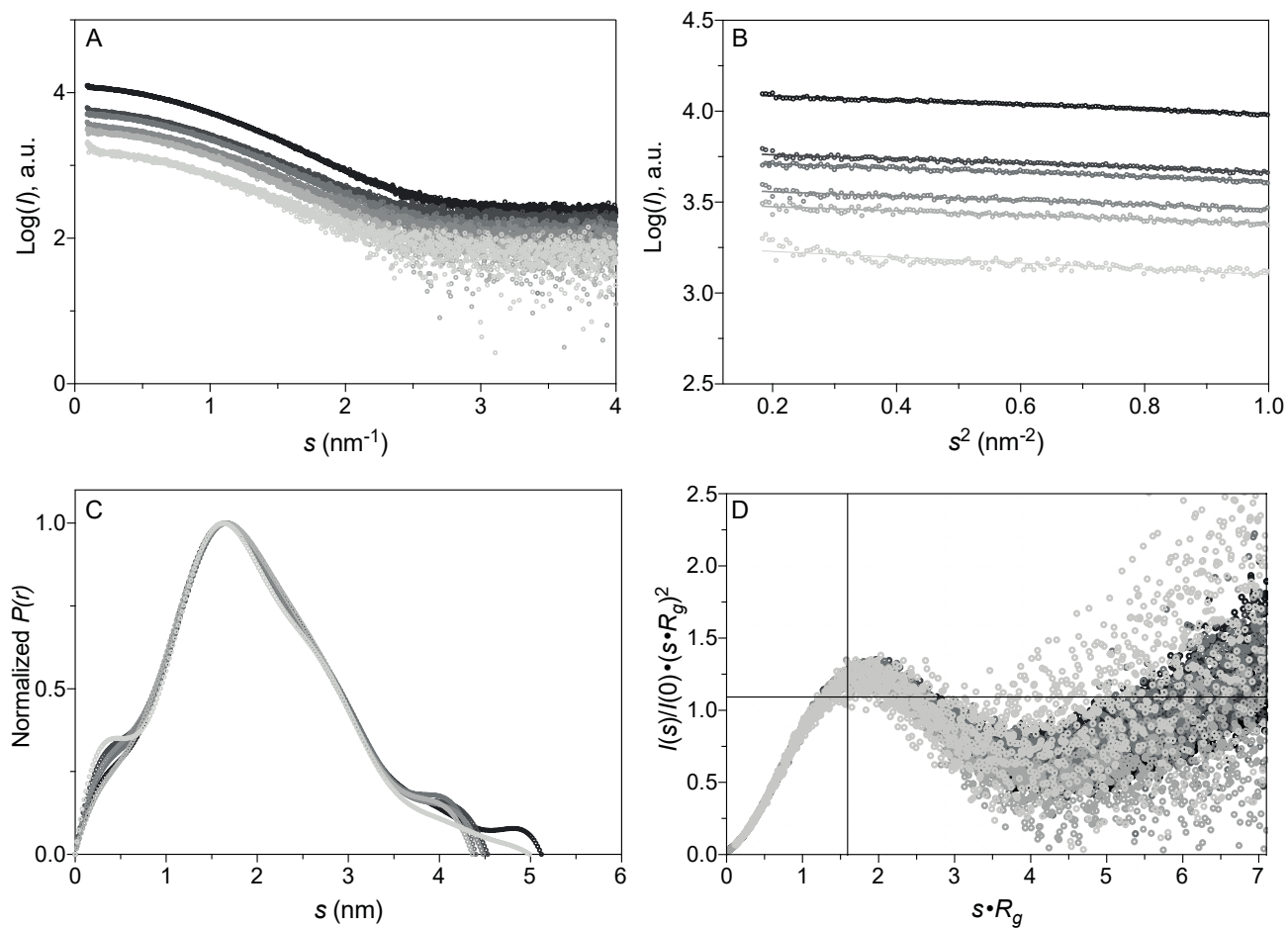


Figure S1. SAXS studies of AtTAF4-RST. (A) SAXS scattering curves of AtTAF4-RST at different concentrations from light gray (1.12 g/L) to black (8.93 g/L). Parameters from the experiments are presented in Table S1. (B) Guinier plots and (C) normalized pair distance distribution, $P(r)$. (D) Dimensionless Kratky plot representations of the scattering data at different concentrations.

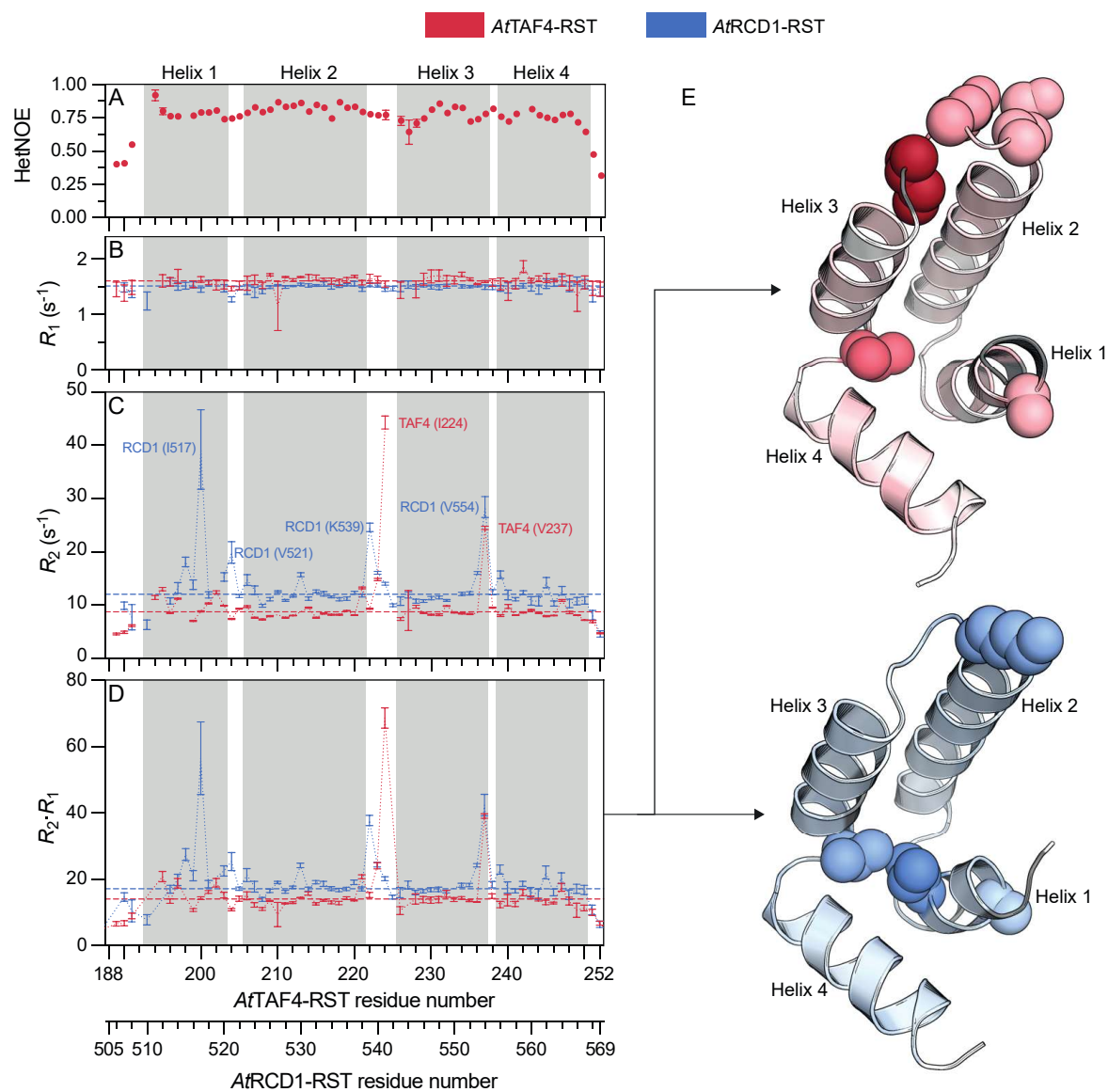


Figure S2. Dynamics of *AtTAF4-RST* compared to *AtRCD1-RST*. (A) ^1H - ^{15}N HetNOEs for *AtTAF4-RST*. (B) ^{15}N longitudinal relaxation rates for *AtTAF4-RST* (red) and *AtRCD1-RST* (blue) (from (1)), the dashed lines indicate the trimmed mean value of residues in secondary structures. (C) Transverse relaxation rates. (D) Relaxation rate products. Grey background indicates helical structure in *AtTAF4-RST*. (E) Relaxation rate products highlighted on the structures of the two RST domains. Residues drawn as spheres differ significantly based on a mean + 1 standard deviation criteria.

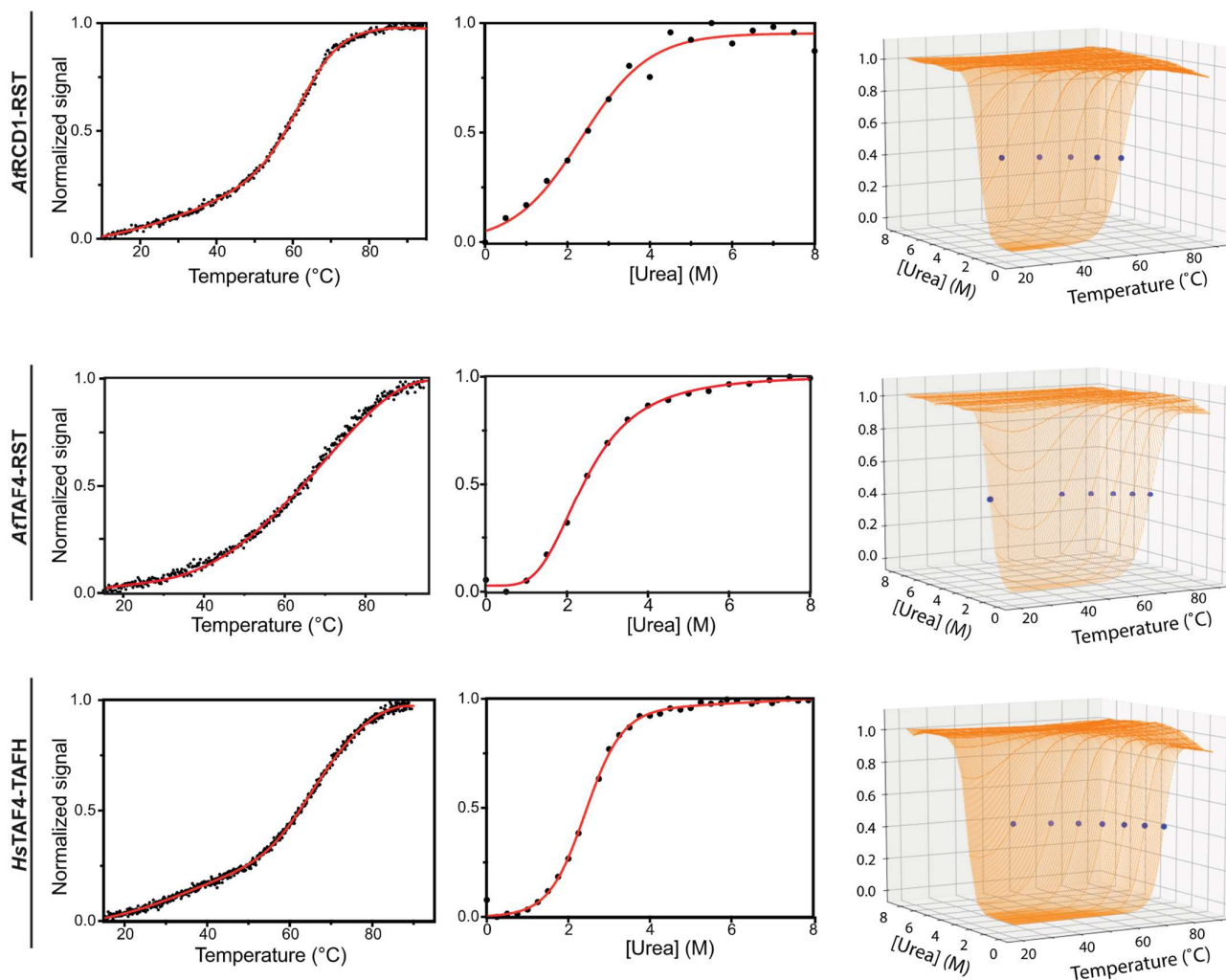


Figure S3. Stability measurements of the *AtRCD1-RST*, *AtTAF4-RST* and *HsTAF4-TAFH* domains.

Normalized signal from CD spectroscopy (222 nm) of 0.1 mg ml^{-1} protein domain in 20 mM sodium phosphate, pH 7.4, as in function of temperature (left) and urea concentration (middle), or from fluorescence detected unfolding using by two-dimensional global analysis (right) of the domains recorded in sodium phosphate buffer, pH 7.4 at $60 \mu\text{M}$ protein concentration. The blue circles correspond to the transition point of the curves.

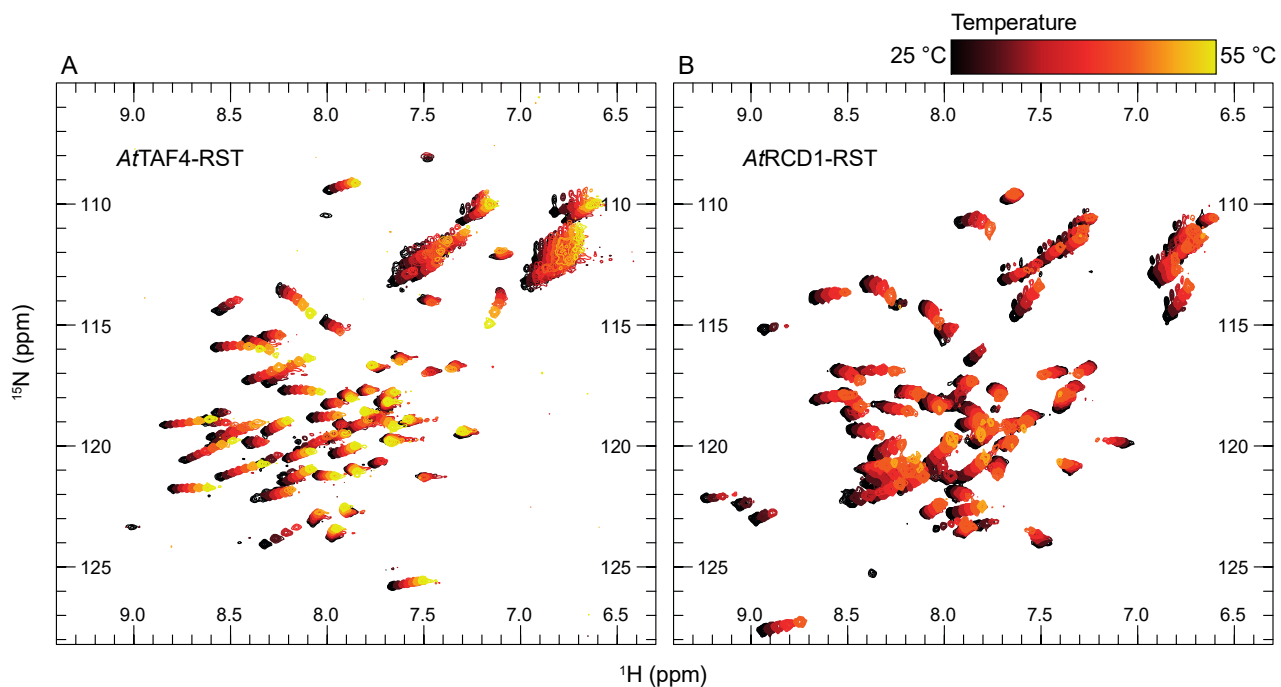


Figure S4. HSQC spectra of thermal unfolding of RST from *AtTAF4* and *AtRCD1*. ^{15}N , ^1H HSQC spectra of ^{15}N -labeled *AtTAF4*-RST (A) and *AtRCD1*-RST (B) recorded in 5 °C intervals from 25 °C (black) to 55 °C (yellow). No *AtRCD1*-RST peaks could be resolved at 55 °C.

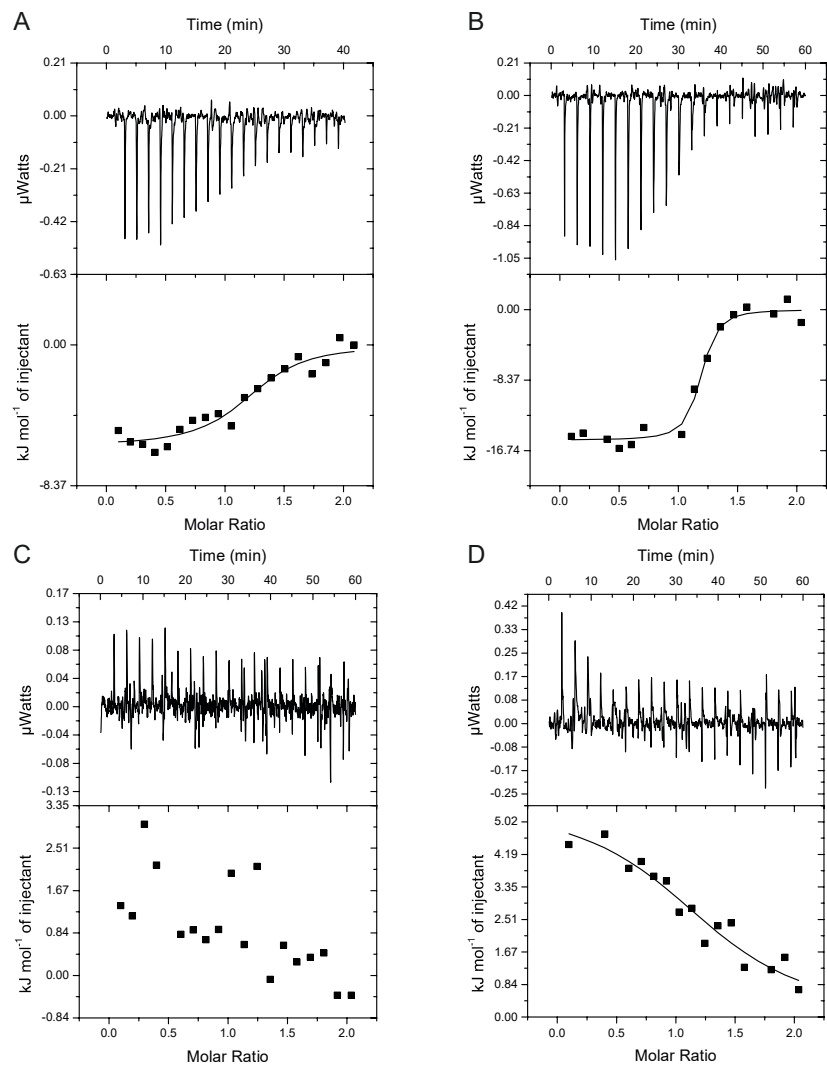


Figure S5. ITC measurements at different temperatures. ITC data showing the titration of (A) *At*TAF4-RST into *At*DREB2A at 25 °C, (B) *Hs*TAF4-TAFH into *At*DREB2A at 25 °C and (C) *At*TAF4-RST into ANAC013 at 25 °C and (D) at 10 °C. In each panel, the upper half shows baseline-corrected raw data from the titration and the lower half shows the normalized integrated binding isotherm together with the binding curve fitted to a one-site binding model.

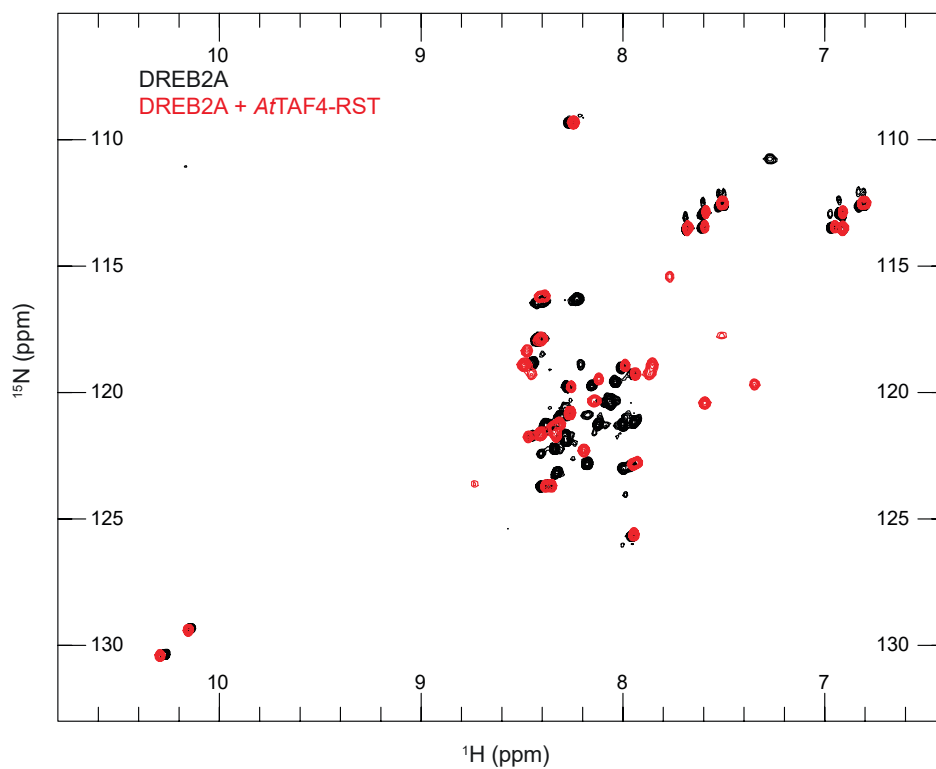


Figure S6. HSQC spectra of free and *AtTAF4-RST* bound DREB2A. $^{15}\text{N},^1\text{H}^{\text{N}}$ HSQC spectra of ^{15}N -labeled DREB2A₂₄₃₋₂₇₂ in the free state (black) and the *AtTAF4-RST* bound state (red). Two tryptophan sidechain peaks are visible in both states around 10 ppm, this is due to the presence of a Trp-Pro motif which has an increased population of the *cis* isoform.

References

1. Staby, L., Due, A. D., Kunze, M. B. A., Jørgensen, M. L. M., Skriver, K., and Kragelund, B. B. (2021) Flanking Disorder of the Folded $\alpha\alpha$ -Hub Domain from Radical Induced Cell Death1 Affects Transcription Factor Binding by Ensemble Redistribution. *Journal of Molecular Biology*. **433**, 167320